

Skin colour detection under changing lighting conditions

Moritz Störring, Hans J. Andersen, and Erik Granum* **

Laboratory of Image Analysis, Aalborg University
 Fredrik Bajers Vej 7D
 DK-9220 Aalborg East
 Denmark

Abstract. Skin colour detection is an often used cue in human motion tracking, especially in face tracking. Skin colour detection is orientation invariant and fast to process. In this paper skin colour is modelled based on a reflectance model of the skin, knowledge about the camera parameters, and the spectrum of the light source. In particular, the location of the skin colour area in the chromaticity plane is estimated for different light sources, given known camera characteristics. The model is empirically validated. It has application in adaptive segmentation of skin colour and may have application in the estimation of the colour temperature in camera images containing skin colour.

1 Introduction

One aim of computer vision research is to develop robust techniques to automatically detect and track objects. An important field of object tracking is human face tracking, which is used in applications as different as human computer interfaces, surveillance systems, or automatic camera men.

The segmentation of skin colour is an often used feature in face tracking systems [1, 2, 3, 4]. It is mostly used as a first approximate localisation and segmentation of faces in the camera image, in order to reduce the search area for other more precise and computationally expensive facial feature detection methods. Advantages of using skin colour are that it is orientation invariant, and one of the faster facial feature detection methods. It is therefore suitable for real time systems [2].

A problem with robust skin colour detection arises under varying lighting conditions. The same skin area appears as two different colours under two different lighting conditions. This is a general problem in colour vision, called *colour constancy*. The skin colour appearance depends on the brightness and the colour temperature of the light source. The dependency on the brightness can be resolved by transforming into a chromatic colour space as done by, e.g., Yang and Waibel [2]. The dependency on the colour temperature of the lighting is not usually taken into account in skin colour detection, despite the fact that the location of the skin colour area changes drastically in the chromaticity plane when changing the colour temperature of the lighting.

This paper investigates the image formation process and in particular, evaluates the consequences of varying the light source colour temperature on the appearance of the skin colour. A skin colour model, which was recently proposed by Ohtsuki and Healey [5], is adapted to estimate the location of the skin colour cluster in the chromaticity plane using knowledge about the skin reflectance, the light source, and the used camera. The model is validated with images containing skin taken under artificial lighting with different correlated colour temperatures. The skin colour model can be used to limit the search area in the chromaticity plane and also for adaptive skin colour segmentation under changing light conditions which are present in non-constraint environments. Furthermore, using the model it might be possible to estimate the current colour temperature if the image contains skin colour and, for example, readjust the white balance of the camera.

In the following sections the skin colour model will be described, results of model validation will be presented and discussed, and future application of the model will be illustrated.

* Email: {mst,hja,eg}@vision.auc.dk

** This work was supported by the European Communities TMR research network SMART II, contract no. ERBFMRX-CT96-0052

2 Modelling Image Formation

The image formation process using a colour video camera can be described by spectral integration. Knowing the spectrum of the incoming light, the spectral sensitivity of the sensing elements, and the spectral transmittance of filters in front of the sensing element one can model the RGB values. The incoming light results from the spectrum of the light source and the reflectance characteristic of the reflecting material, which is described by the Dichromatic Reflection Model. In this work human skin is the reflecting material. In the following subsections the above mentioned process will be described and the location of the skin colour in the chromaticity plane will be calculated for light sources with different colour temperatures.

2.1 Dichromatic Reflection Model

The Dichromatic Reflection Model describes the light L , which is reflected from a point on a dielectric, nonuniform material as a mixture of the light $L_{Surface}$ reflected at the material surface (*surface reflection*) and the light L_{Body} reflected from the material body (*body reflection*):

$$L = L_{Surface} + L_{Body} \quad (1)$$

The light reflected on the surface has approximately the same spectral power distribution as the light source. The light which is not reflected at the surface penetrates into the material body where it is scattered and selectively absorbed. Some fraction of the light arrives again at the surface and exits the material. The light travelling through the body is increasingly absorbed at wavelengths that are characteristic for the material. The body reflection provides the characteristic object colour [6].

2.2 Skin Reflectance

This subsection summarises the method to synthesise skin reflectance spectra reported by Ohtsuki and Healey [5]. In the proposed model the human skin is described by its thin surface layer, the *epidermis*, and its thicker layer placed under the *epidermis*, the *dermis*. The *surface reflection* of the human skin takes place at the *epidermis* surface. It is approximately $\rho_{Surface} = 5\%$ independent of the lighting wavelength and independent of the human race [7]. The rest of the incident light (95%) is entering the skin where it is absorbed and scattered within the two skin layers. This process was referred to as *body reflectance* in the Dichromatic Reflection Model. The scattering in the *epidermis* is considered negligible. The *epidermis* mainly absorbs light, hence it has the properties of an optical filter. The light is transmitted depending on its wavelength and the *dopa-melanin* concentration in the *epidermis*. In the *dermis* the light is both scattered and absorbed. The absorption is mainly due to the ingredients in the blood such as *haemoglobin*, *bilirubin*, and *beta-carotene*. The optical properties of the *dermis* are basically the same for all human races. The skin colour is thus determined by the *epidermis* transmittance which depends mainly on the *dopa-melanin* concentration. The body reflectance ρ_{Body} is given in equation 2. The *epidermis transmittance* is squared because the light passes twice through it - when entering and when leaving the body. In the model the transmittance of *dopa-melanin* is used for the *epidermis transmittance*.

$$\rho_{Body} = \langle \textit{epidermis transmittance} \rangle^2 + \langle \textit{dermis reflectance} \rangle \quad (2)$$

Figure 1 (left) shows three spectral reflectance curves of human skin [7, 8]. The uppermost is representative for normal Caucasian skin, the middle one for Caucasian skin right after sunburn (*erythematous*), which gives the skin a reddish appearance, and the lower one for Negro skin. The uppermost corresponds to a low blood content in the *dermis* whereas the middle one corresponds to a high blood content. Given these spectral reflectance curves and the transmittance of *dopa-melanin*, it is possible to synthesise spectral reflectance curves for any *dopa-melanin* concentration as shown in figure 1 (right). In other words the two spectral reflectance curves of Caucasian skin in figure 1 (left) enclose the range of the blood content (reddish appearance of the skin) of the *dermis*. They are used to generate the spectral reflectance curves of skin with different brightnesses (figure 1 right).

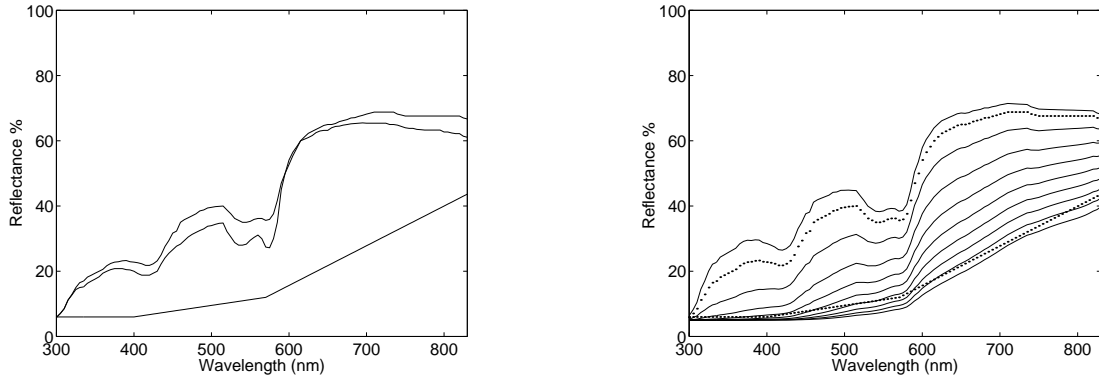


Fig. 1.: Left: Spectral reflectance curves of human skin for normal Caucasian [7], erythematous Caucasian [7], and dark Negro skin [8]. Right: Synthesised spectral reflectance curves using the uppermost curve of the left figure. The dotted curves are the measured skin reflectance of Caucasian and dark Negro skin, respectively, shown in the left figure.

2.3 Light Spectra and Colour Temperature

The colour appearance of an object is determined by its reflectance and the light it is exposed with. The previous subsection showed the spectral reflectance curves of human skin. This subsection presents light spectra of artificial light sources (figure 2). The properties of light spectra can be described by their *correlated colour temperature* (CCT) and the *general colour rendering index* R_a [9]. The spectrum of a light source with a low CCT has a maximum in the radiant power distribution at long wavelengths, which gives the material a reddish appearance. Examples are sunlight during sunset and artificial light sources such as low power electric light bulbs. A light source with a high CCT has a maximum in the radiant power distribution at short wavelengths and gives the material a bluish appearance, e.g., skylight in the early morning and special fluorescent lamps. The general colour rendering index of a light source determines the quality of the colour appearance of objects in comparison with their appearance under a reference light source - the higher R_a the better the correspondence. R_a can maximally be 100 [8]. Fluorescent lamps can have low values for R_a , thus the object will have a unnatural colour appearance. Electric light bulb have mostly tungsten as material for making the filaments. The spectral radiance of tungsten is approximately like that of a Blackbody radiator (figure 2 left) which has $R_a = 100$.

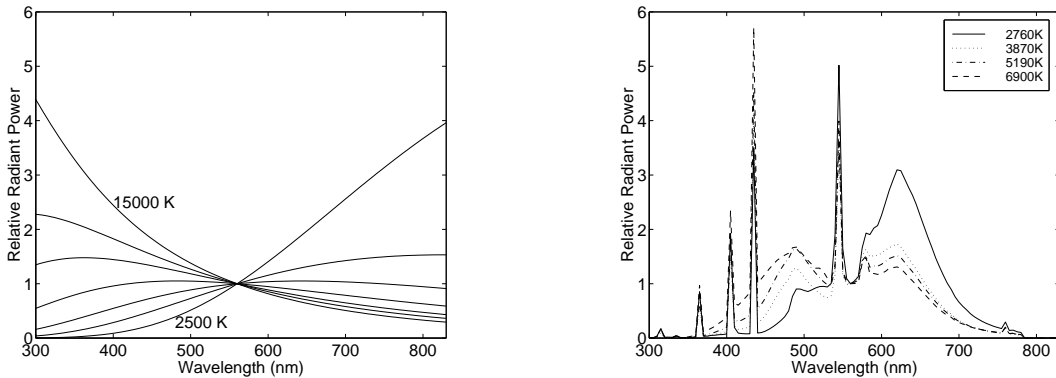


Fig. 2.: Relative radiant power distributions normalised at $\lambda = 560\text{nm}$. Left: Blackbody at $T=2500\text{K}$ to 15000K [8]. Right: Fluorescent lamps (Philips TLD) CCT= 2760K, 3870K, 5190K, and 6900K, $R_a > 90$.

2.4 Spectral Integration

The measured image data is influenced by the characteristics of the camera. While the Dichromatic Reflection Model describes light reflection using the continuous light spectrum, the camera sensing device uses only a finite set of samples to describe the spectrum [6]. Sample measurements are obtained by filtering the light spectrum and integrating over the filtered spectrum, which is referred to *spectral integration*:

$$R = \int_{\lambda} E(\lambda)\rho_{skin}(\lambda)f_R(\lambda) d\lambda, \quad G = \int_{\lambda} E(\lambda)\rho_{skin}(\lambda)f_G(\lambda) d\lambda, \quad B = \int_{\lambda} E(\lambda)\rho_{skin}(\lambda)f_B(\lambda) d\lambda \quad (3)$$

where $E(\lambda)$ is the spectrum of the light source, $\rho_{skin}(\lambda)$ the skin reflectance, and $f_{R,G,B}(\lambda)$ the spectral sensitivities of the red, green, and blue sensing elements of the camera, figure 3. Using the red, green, and blue sensing elements reduces the infinite vector space to a three-dimensional space, called the *colour space*, often represented by RGB.

A material appears white if its spectral reflectance is constant one over all visible wavelength $\rho(\lambda) = const = 1$. From equation 3 and the different light spectra in figure 2 one can see that the ratio between R, G, and B will change when changing to a light source with another spectrum and by that another CCT. That is why colour video cameras have to be white balanced whenever the CCT changes. Video cameras may be white balanced by taking an image of a surface with $\rho(\lambda) = 1$, e.g., Barium Sulphate, and then adjusting the three colour channels such that $R = G = B$.

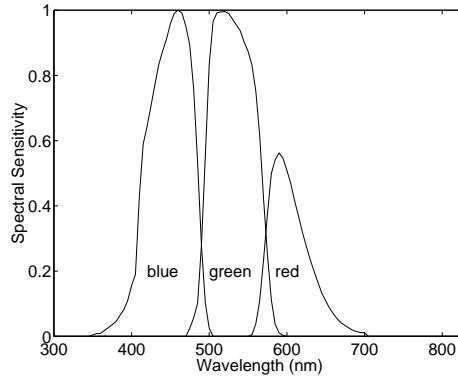


Fig. 3.: Spectral sensitivities (*tristimulus characteristic*) of the JAI M90 3CCD colour video camera.

2.5 Skin Colour Location in the Chromaticity Plane

Using the model described in the previous subsections it is possible to estimate the location of skin colour in the chromaticity plane. The chromaticities red and green are calculated as follows:

$$red = \frac{R}{R + G + B} \quad green = \frac{G}{R + G + B} \quad (4)$$

Figure 4 (left) shows the skin colour area in the chromaticity plane given the light source is a Blackbody radiator with $T = 3200K$ and the camera is white balanced to the same light source. The location of the light source is marked with the triangle. Every dot of the skin area is calculated by spectral integration over one of the synthesised spectral reflectance curves in figure 1, equation 3, and then using equation 4 to calculate the chromaticities. The square denotes the mean value of the skin colour area. In figure 4 (right) the camera is white balanced to a Blackbody radiator $T = 3200K$. The two loci, light source and body reflectance, show where Blackbody light sources for different colour temperatures (upper) and the respective mean values of the skin area (lower) are located in the chromaticity plane. It can be seen that that small changes of the lighting CCT around the camera white balance CCT result in large changes of the skin colour location in the chromaticity plane.

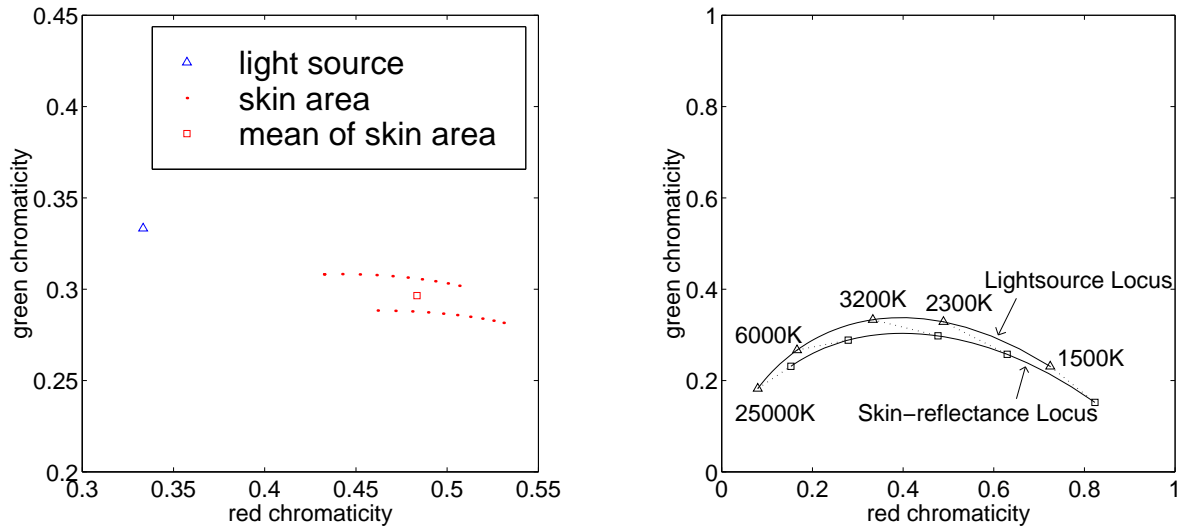


Fig. 4.: Left: Calculated location of light source and skin colour area in the chromaticity plane for a Blackbody radiator light source with $T=3200\text{K}$ and a camera which is white balanced to the same light source. Right: Light sources and mean values of skin colour areas for different colour temperatures if the camera is white balanced to a Blackbody radiator of $T=3200\text{K}$.

3 Image Acquisition

For the empirical validation of the skin colour model images are taken from faces of seven subjects under lighting with different correlated colour temperatures. The setup for capturing these images is described in this section.

The images are captured with a JAI M90 3CCD colour video camera equipped with a Fudjinon wide angle lens and connected to a Silicon Graphics Sirius frame-grabber. The automatic gain control is switched off and the gamma correction is set to one. The lens opening and the shutter speed are manually adjusted to make use of the dynamic range of the camera. The spectral sensitivity, called *tristimulus characteristic*, of the M90 camera is shown in figure 3.

Fluorescent lamps serve as light sources during the image acquisition. Four different correlated colour temperatures are used: CCT = 2760K, 3870K, 5190K, and 6900K (Philips TLD 927, TLD 940, TLD 950, TLD 965). The spectra of these lamps are provided from Philips (see figure 2). The lamp casings are from Louis Poulsen, model Tommy, which have an efficient reflector and high frequency lamp control gears ($> 24\text{kHz}$) in order to acquire flicker free light. For each CCT four 58W lamps are used. Figure 5 shows the setup for the image acquisition and a typical image taken by this setup. JAI recommends for the M90 camera a standard illumination of 2000 lux using an opening of $F=5.6$. This illumination is available in approximately 1.5 meter distance to the lamps. Fluorescent lamps provide their full luminous flux approximately 20 minutes after they are switched on. Therefore all the lamps are switched on during the acquisition of a set of images of one subject and are covered by a box so that only lamps with the same CCT give light at a time. The camera is white balanced to the fluorescent lamp with a CCT of 3870K.

Indoor images from seven subjects coming from a variety of countries (China, Iran, Cameroun, Latvia, Greece, Denmark, and India) and hence with different skin colours were taken showing their faces, as illustrated in figure 5. Five images of each subject were taken using the lamps in the order CCT = 3870K, 2760K, 6900K, 5190K, 3870K. Two images are taken at the CCT = 3870K, one at the beginning and one at the end of a set of images as a reproducibility test to make sure that the subject's skin properties did not change, e.g., less reddish at the end of the sequence.

4 Model Verification

This section presents a qualitative comparison of the measured and modelled skin colour areas in the chromaticity plane. The images, acquired as described in the previous section, were hand segmented into skin

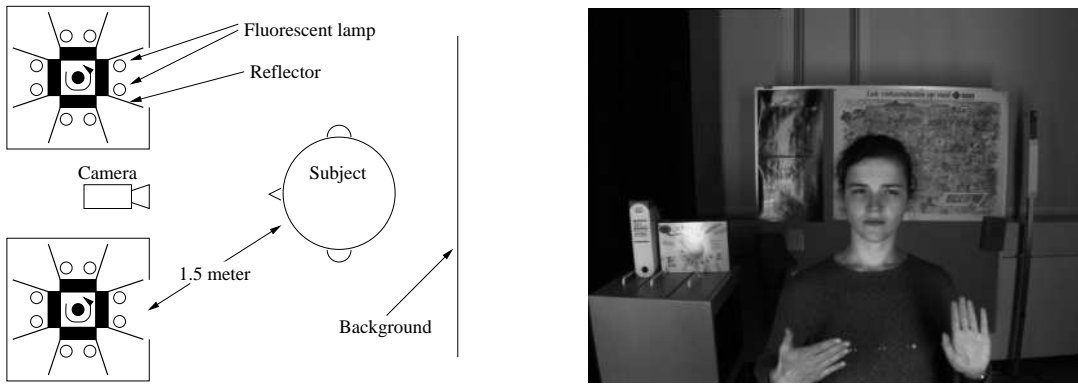


Fig. 5.: Left: Top view of the setup for capturing images of peoples faces under lighting with different CCT. Right: Typical image acquired by the setup shown in the left figure. The image is taken under a CCT of 2760K.

areas and non skin areas. The skin areas are used to calculate the distribution of skin colour in the chromaticity plane.

Figure 6 shows the mean values of the measured skin colour distributions in the chromaticity plane for the seven subjects under the four used CCTs. The solid lines show the skin colour areas calculated by the model for the four CCTs.

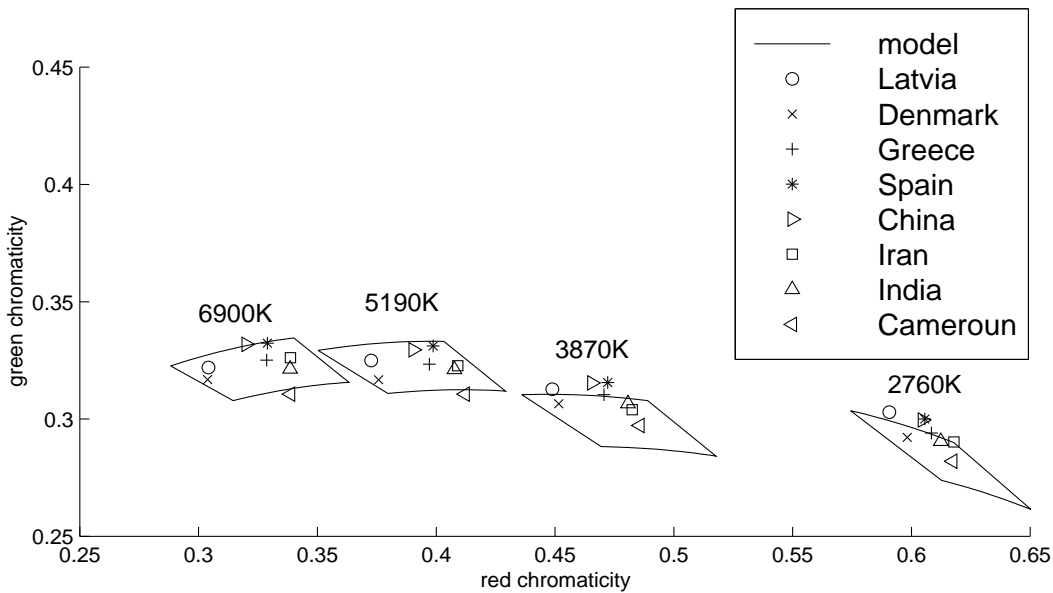


Fig. 6.: Chromaticity plane with modelled skin colour areas and mean values of the measured skin colour distribution under the four different CCT as described in section 3.

The measurements lie inside or near to the modelled skin colour areas. The structure of the distribution of the mean values looks similar for the different CCTs, it changes about the same as the structure of the model changes. The calculated areas for the lower CCTs (2760K and 3870K) are a bit too low in the green component whereas the models for the higher CCTs (5190K and 6900K) are a bit too high in green component.

Figure 7 shows skin colour distributions in the chromaticity plane of Caucasian, Asian, and Negro skin. The camera is white balanced at a CCT = 3870K and the images are also taken under that CCT. Both, the Caucasian and the Asian skin colour distribution seem to be composed of two distributions. A smaller

distribution on the upper left side and a bigger one on the lower right side, see also figure 8 (left). The upper left distributions are probably due to highlights. The solid lines mark the skin area calculated with the model for a wide range of dopa melanin concentration. In figure 7 (left) the upper boundary of the skin colour area is calculated using the body reflectance curves of figure 1. The distributions of the highlights lie outside the calculated skin colour area. If instead a curve for whole skin reflectance is used ([10] p. 175) the highlights are included (see figure 7 right).

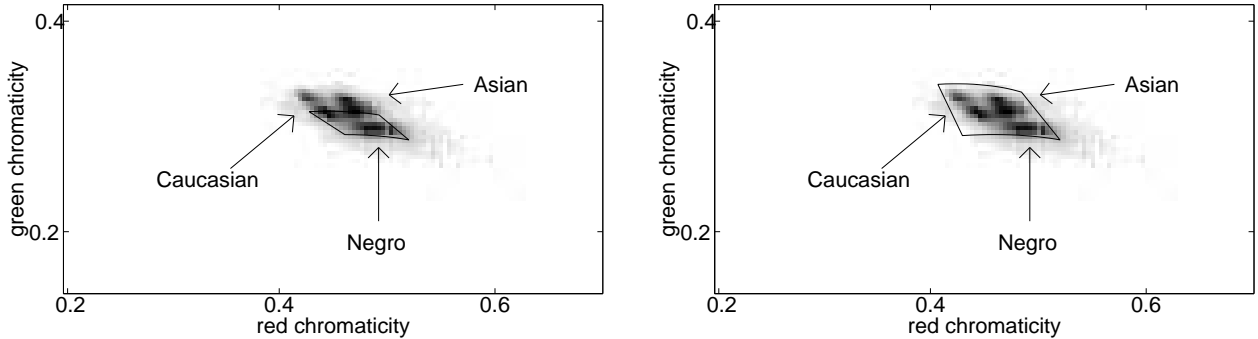


Fig. 7.: Skin colour distribution in the chromaticity plane of images taken at CCT=3870K with a camera white balanced to the same light source. The solid line indicates the skin area, modelled with a large range of dopa melanin. The images contain skin of a Caucasian (Latvia), Asian (China), and Negro (Cameroun). Left: The upper boundary of the skin area is calculated using only body reflectance. Right: The upper boundary of the skin area is calculated using whole reflectance, i.e. considering also highlights.

Figure 8 shows two skin colour distributions in the chromaticity plane under the four CCTs. One distribution is from a light Caucasian subject and one from a Hindu subject. The solid line is the modelled skin area. The models are adapted for each subject by changing the range of dopa melanin concentration and choosing the reflectance curves. The modelling is done for the CCT = 3870K. The skin colour areas for the other CCTs are calculated using the same parameters except the spectrum of the light source, which is changed to the respective one.

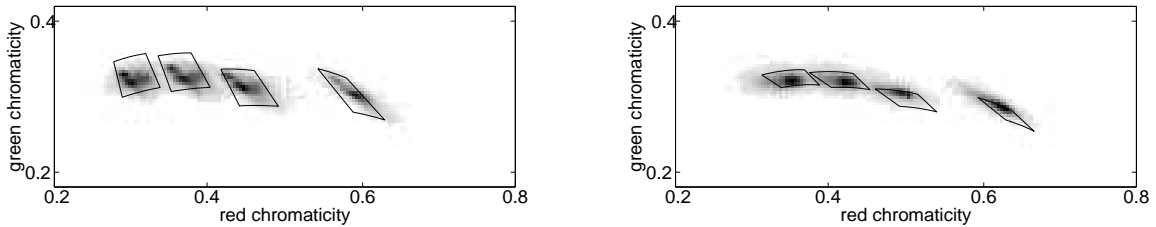


Fig. 8.: Chromaticity plane showing the distribution of skin colour for one subject under changing CCTs. The solid line shows the modelled skin colour area adapted individually at CCT=3870K. Left: Caucasian (Latvia). Right: Hindu (India).

Figure 9 shows the segmentation of the images corresponding to the distributions shown in figure 8 (left) and using the model shown in figure 8 (left).

5 Discussion

By using a physical based model of the skin colour it is possible to calculate the skin colour area in the chromaticity plane for different CCTs. Indoor images of seven people with different skin colours under four different CCTs confirm that the model can be used successfully to detect skin colour in a camera image, given the spectrum of the light source and the camera characteristics are known.



Fig. 9.: Segmented images using the model shown in figure 8 (left). The top left image is the segmentation from the image shown in figure 5.

From figure 6 and figure 8 it can be seen that the measurements and the model for the different CCTs do not fit exactly. With increasing CCT the green component of the model increases more than the green component of the measurements. This effect can be due to the measurement and the modelling. One source of error is in the synthesis of the spectral reflectance curves of human skin which are based on only two Caucasian reflectance curves. Figure 1 (right) shows that the reflectance for Negro skin (dotted line) is smoother than the corresponding synthesised reflectance. The model can probably be improved using real measured reflectance, as given in [8] p. 63. Furthermore, the used spectra of the fluorescent lamps and the tristimulus characteristic of the video camera are product specifications from Philips and JAI, respectively, and not measures of the devices used in this project. In future the spectra of the fluorescent lamps should be measured and real reflectance curves should be used. A quantitative evaluation of the results would then be possible.

The skin colour model may provide the basis for a wide range of applications such as adaptive segmentation of skin colour. If evidence about the presence of a face or skin is given by an other method, e.g., facial feature extraction, it is possible to give an estimation of the current CCT of the lighting. This can be used to adjust the skin colour search area in the chromaticity plane or to automatically adjust the white balance of the camera. The former has applications in surveillance and human computer interfaces under light conditions with large variations. The automatic adjustment of the white balance would be of significance in broadcasting cameras. While these cameras are equipped with sophisticated auto focus and auto iris facilities the white balance is still done manually. The newest broadcasting cameras can be pre-balanced, e.g., for indoors and outdoors and then recognise automatically when they are moved from one light condition to the other. However, they can only switch between the white balance for indoor and outdoor lighting, that means the transition is not continuous. Broadcasting cameras are used for the most part to capture humans and their faces, hence the images contain skin colour which could be used to estimate the current CCT of the lighting. If the difference between the current lighting CCT and the white balance CCT is small ($\Delta CCT < 2000K$) it can be seen from figure 4 (right) that relatively small changes of the lighting CCT

result in large changes of the location of the skin colour area in the chromaticity plane. A reasonable and smooth adjustment of the white balance should therefore be possible.

In future work tests should be done using images from skin in cluttered environments under artificial light, sunlight, and mixed lighting. The latter was recently treated in [11] for two light sources. Skin with other properties than facial skin like the palm of the hands and lips should be investigated.

The images taken for this study were captured in parallel with an 1CCD s-video camera, with and without auto gain control. These images could provide a useful comparison on how the skin colour is distributed if consumer cameras are used.

References

1. Eli Saber, A. Murat Tekalp, Reiner Eschbach, and Keith Knox. Automatic image annotation using adaptive color classification. *Graphical Models and Image Processing*, 58(2):115–126, March 1996.
2. Jie Yang and Alex Waibel. A real-time face tracker. In *Third IEEE Workshop on Applications of Computer Vision*, pages 142–147, Sarasota, Florida, USA, 1996.
3. Stephen J. McKenna, Yogesh Raja, and Shaogang Gong. Object tracking using adaptive colour mixture models. In Roland Chin and Ting-Chuen Pong, editors, *Third Asian Conference on Computer Vision*, number 1, pages 615–622, Hong Kong, China, January 1998.
4. C. Chen and S.-P. Chiang. Detection of human faces in colour images. *IEE Proc.-Vis. Image Signal Process*, 144(6), December 1997.
5. Tomoyuki Ohtsuki and Glenn Healey. Using color and geometric models for extracting facial features. *Journal of Imaging Science and Technology*, 42(6):554–561, December 1998.
6. Gudrun Klinker. *A Physical Approach to Color Image Understanding*. A K Peters, Ltd, 289 Linden Street, Wellesley, MA 02181, 1993.
7. R. R. Anderson, J. Hu, and J. A. Parrish. Optical radiation transfer in the human skin and applications in in vivo remittance spectroscopy. In R. Marks and P. A. Payne, editors, *Bioengineering and the Skin*, chapter 28, pages 253–265. MTP Press Limited, 1981.
8. Günter Wyszecki and W. S. Stiles. *Color Science: Concepts and Methods, Quantitative Data and Formulae*. John Wiley and Sons, 1982.
9. Anonymous. Method of measuring and specifying colour rendering properties of light sources. Technical Report CIE 13.3, Commission Internationale de L'Eclairage (CIE), 1995.
10. R. R. Anderson and J. A. Parrish. *The Science of Photomedicine*, chapter Optical Properties of Human Skin, pages 147–194. Plenum Press, 1982.
11. H. J. Andersen and E. Granum. Classifying illumination condition from two light sources by colour histogram assessment. submitted for: *Journal of Optical Society of America A*, March 1999.